Available online at www.sciencedirect.com
SCIENCE DIRECT®
ELSEVIER
Applied Surface Science 246 (2005) 174–182
applied surface science
www.elsevier.com/locate/apsusc

Formation of vacancy islands tailored by Pt nanocrystallites and Ar^+ sputtering on TiO_2(1 1 0) surface

A. Berkó*, A.M. Kiss, J. Szökő

Reaction Kinetics Research Group of the Hungarian Academy of Sciences, University of Szeged, Dom ter 7, P.O. Box 168, H-6701 Szeged, Hungary

Received 27 August 2004; received in revised form 3 November 2004; accepted 3 November 2004
Available online 8 December 2004

Abstract

The effect of Ar^+ bombardment was studied on TiO_2(1 1 0)-(1 × *n*) surface decorated with Pt nanoparticles by scanning tunnelling microscopy (STM). Pt crystallites were fabricated in a large separation by the so-called seeding + growing method described earlier [A. Berkó, G. Klivényi, F. Solymosi, J. Catal. 182 (1999) 511]. It was shown that the presence of Pt crystallites results in an enhanced sputtering of the support in the vicinity of the particles at high temperatures. This process causes a dramatic increase in the average corrugation of the substrate and leads to formation of deep nanoditches in the orientation of [0 0 1]. The analysis of the geometry of the nanoparticles revealed that they are decorated with the material of the support. The noble metal nanocrystallites grown in large separation are suitable for the visualization of the accelerated surface diffusion and sputtering in the region around the crystallites. The phenomenon presented here prompts a nanotechnological tool capable of fabricating nanopits in tailored distribution (in the range of 5–200 nm) that is determined by the original Pt nanoparticles formed on the TiO_2(1 1 0) surface.
© 2004 Elsevier B.V. All rights reserved.

Keywords: Pt nanoparticles; TiO_2(1 1 0) support; Scanning tunnelling microscopy; Ar^+ bombardment; Tailored distribution of nanopits

1. Introduction

Self-organized formation of periodic nanoscale structures induced by ion bombardment at different temperatures is a very promising method in the recent nanotechnology [1–4]. These works have largely contributed to the deeper insight into the phenomena connected both to the surface diffusion and the formation of reduced dimensional (0D, 1D, 2D) nanoobjects. For this type of studies, the scanning tunnelling microscopy (STM) is a very appropriate method by which a tremendous development was recently achieved in the construction of nanoscale material systems of technological importance [5].

The 2D model – Pt nanoparticles supported on TiO_2(1 1 0) surface – studied in the present paper is a

* Corresponding author. Tel.: +36 62 544 646; fax: +36 62 420 678.
E-mail address: aberko@chem.u-szeged.hu (A. Berkó).

0169-4332/$ – see front matter © 2004 Elsevier B.V. All rights reserved.
doi:10.1016/j.apsusc.2004.11.004

well known SMSI (strong metal–support interaction) system where the high temperature thermal treatment results in the decoration (encapsulation) of Pt nanoparticles by the reduced species of the support material [6–8]. Research is in progress to understand this phenomenon on the atomic scale [9,10]. During the work on the Pt/TiO_2(1 1 0) model catalysts we have experienced that Ar^+ bombardment used customarily to clean the surface or to remove the metal particles causes a strong roughening of the flat samples. This phenomenon is studied in detail in this work. In an earlier study a special method was developed for growing noble metal nanoparticles on the TiO_2(1 1 0) surface in large separation [11–13]. This configuration makes it possible to follow the metal–support interaction for a single nanoparticle, or in other words, for that particle which has negligible interaction with the neighbouring ones.

2. Experimental

The experiments were carried out in an UHV chamber equipped with a commercial room temperature STM head (WA-Tech), a DP-CMA electron energy analyzer (STAIB) for AES and a quadrupole mass spectrometer (BALZERS) for gas analysis. The polished TiO_2(1 1 0) single crystal samples of 5 mm × 5 mm × 1 mm size were purchased from PI-KEM. The probe was sticked onto a Ta-plate and heated by a W-filament from the rear side. The temperature was measured by K-type (chromel–alumel) thermocouple fixed to the side of the sample by ceramobond-571 (AREMCO). The cleaning procedure consisted of annealing at 900 K in UHV for a few days, several cycles of Ar^+ sputtering (1.5 keV, 3×10^{15} ion cm^{-2} min^{-1}, 10 min) and post-annealing for a few minutes at 1100 K. The samples were moved by an UHV-compatible transfer system from the STM-head to the central manipulator where the different treatments of the sample were performed. A side vacuum chamber served for changing of the probes. The vacuum system was evacuated by ion-getter and turbomolecular pumps in order to achieve an ultimate pressure of 5×10^{-8} Pa.

Pt was deposited by resistive heating of a high purity (99.95%) Pt filament. The rate of the evaporation was controlled by adjusting the filament current. The cleanness of the sample surface and the ultrathin metal adlayer was checked by Auger-electron spectroscopy. The Pt coverage is expressed in monolayer equivalent (ML), which corresponds to 1.6×10^{15} atom cm^{-2}. The actual coverage was calculated by the determination of the total volume of the well-separated 3D metal nanoparticles formed on the effect of annealing at 1100 K. It should be remarked that this method might contain some systematic error because of the encapsulation or/and sinking of the supported nanoparticles; nevertheless these effects may cause an error less than 20–30% in our case [6].

For the STM imaging, chemically edged W tips were applied and sharpened 'in situ' above the TiO_2 surface by applying 5–10 V pulses. The characteristic images shown in this work were chosen from numerous records obtained on different regions of the sample. Most of the presented images are electronically untreated records; only some of them were gently smoothed. The systematic Ar^+ sputtering was performed with the same ion gun as the cleaning. The total current flowing through the sample was measured during the treatment and it was applied for calculation of the ion dose. The incident angle of the ion beam was approximately 60° in all experiments.

3. Results and discussion

The clean TiO_2(1 1 0) surface used in this work exhibited characteristic added rows running in the [0 0 1] crystallographic orientation on the large atomic terraces which were separated by steps mostly of [0 0 1] and [1 1 0] direction (Fig. 1A). The size of the images in Fig. 1 is 100 nm × 100 nm. It is worth mentioning that the surface density of the 1D structures varied slightly with the duration of the annealing of the sample at 1100 K. More generally, the actual morphology of the probe depended on the past of it. The sizes of the terraces are apparently rather large (typically 50 nm × 100 nm). The texture of the lower terraces in the vicinity of the [1 1 0] steps exhibited (1 × 2) arrangement where the outrising 1D strings were separated by 1.30 nm. The other parts of the terraces can be identified as (1 × n) reconstructed structure where the regions between the rows exhibited a bulk terminated (1 × 1) arrangement (not seen at this magnification). The more detailed description and

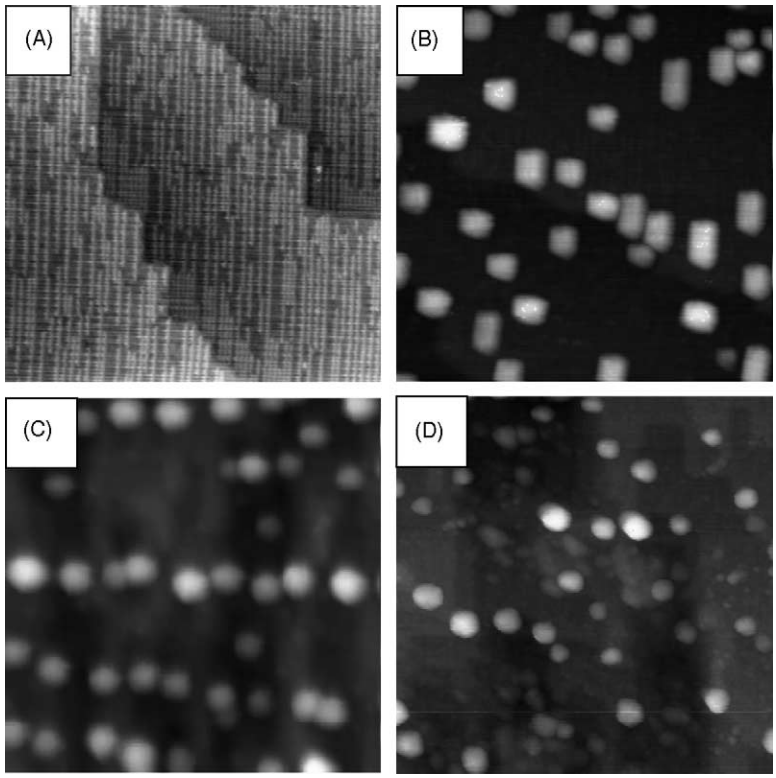

Fig. 1. Characteristic STM images of 100 nm × 100 nm size recorded (A) on the clean TiO_2(1 1 0)-(1 × n) surface and (B) after the fabrication of Pt nanocrystallites by the so called 'seeding + growing' method (see text). The effect of the Ar^+ bombardment (1.5 keV, 3×10^{15} cm^{-2} min^{-1}) of the Pt-decorated TiO_2(1 1 0)-(1 × n) surface at 1100 K: duration of (C) 1 min and (D) 12 min.

the identification of the structural features of this widely studied surface can be found in numerous works and in the cited references as well [14–20].

Fig. 1B shows the characteristic morphology of the TiO_2(1 1 0)-(1 × n) surface mapped after the deposition of 0.01 ML Pt at 300 K followed by annealing at 1100 K for 10 min ('seeding') and post-exposure to Pt (0.56 ML) at 1100 K ('growing'). This method applied for the growing of metal nanoparticles in large separation was worked out in our laboratory and published earlier in detail [11–13]. It can be seen that the particles are distributed rather uniformly and the average diameter of the crystallites varies in the range of 8–10 nm. The supported Pt particles are typically located at the steps or, more exactly, at the cross points of two different steps. It should be remarked that the surface concentration of the seeds could be varied by fine-tuning of the amount of the deposited metal in the seeding step. In harmony with our earlier measurements, the surface density of the nanoparticles (seeds) increases almost linearly with the metal coverage in the range of 0.001–0.050 ML. In the second part of the fabrication of well-separated nanocrystallites, additional metal was exposed at 1100 K. The amount of the deposited metal was estimated from the total volume of the particles and it is given in the so-called monolayer equivalent (ML) unit. In our case, the size-distribution of the particles is rather narrow, the shape of the particles is also very similar and all of them are oriented with one side along the [0 0 1] direction of the support (Fig. 1B). The nanocrystallites exhibit mostly (approximately 80%) a hexagonal outline with flat (1 1 1) top facets declined by 5–6° to the terrace plane of the support, at the same time some particles are strongly elongated in the surface orientation of [0 0 1] and some others exhibit a square (1 0 0) top facet. The largest crystallites contain approximately 7–8 Pt-layers. The STM images and the tunnelling spectra recorded on the

top of the crystallites (not presented here) have shown that an insulator overlayer is formed. This feature can be explained by the decoration of the particles by some TiO_x phase. This behaviour is well known for the so-called SMSI (strong metal–support interaction) systems where the support is a reducible oxide and the supported metal is some kind of noble metal [6–10].

The effect of Ar^+ sputtering of this surface was followed by STM. Fig. 1C shows a characteristic region of 100 nm × 100 nm size recorded after 1 min sputtering at 1100 K. The most important change is the tremendous increase of the corrugation in the areas of the same size, before and after the treatment this parameter increased from 2.8 to 6.0 nm calculated from the images B and C, respectively. (The corrugation measures the z difference between the lowest and the highest point in a given area). It is important to emphasize that all of the images presented in the figures have been chosen from many other pictures in order to characterize the main morphological changes. The second important observation is the transformation of all of the particles into a round shape form. The third important feature is the appearance of nanoditches in the support surface. The main orientation of these new structures is [0 0 1]. Further Ar^+ bombardments of the surface result in a gradual decrease of the average size of the particles. Fig. 1D shows the characteristic morphology after the ion treatment of 12 min. The particle size decreased down to 3–5 nm, the total volume of the particles dropped to approximately 80% of the original value. The corrugation is 4.3 nm in this latter case.

In Fig. 2 the change of the total volume of the particles and the corrugation (based on 100 nm × 100 nm area, approximately 40 particles seen in Fig. 1B and C) are plotted as the function of the duration of the Ar^+ bombardment. The values plotted in the figure were calculated on the basis of the STM

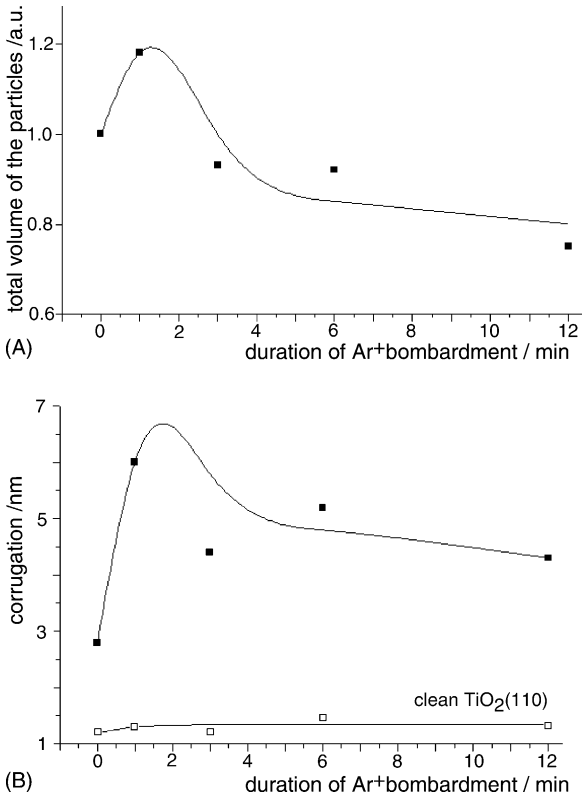

Fig. 2. The effect of the duration of Ar^+ treatments at 1100 K on the Pt-decorated $TiO_2(1\ 1\ 0)$-$(1 \times n)$ surface characterized by the image in Fig. 1B: (A) the change of the total volume of the adparticles; (B) the change of the corrugation of the recorded images of 100 nm × 100 nm. The effects of the same ion treatments were plotted also for the clean $TiO_2(1\ 1\ 0)$-$(1 \times n)$ surface (bottom of the figure).

images (not all presented) recorded after the given sequence of the Ar^+ treatment. The surprising enhancement of the volume of the particles (approximately by 20%) is accompanied by a dramatic increase of the corrugation (from 2.8 up to 6.0 nm) in the early stage of the bombardment. Further sputtering results in a gradual decrease in both of the total volume of the particles and the average corrugation of the surface. These latter changes clearly indicate that the adparticles are gradually removed from the support in harmony with the expectations. In the lower part of Fig. 2B the effect of the same Ar^+ bombardment is plotted for a clean TiO_2(1 1 0) surface. It can be seen that the original

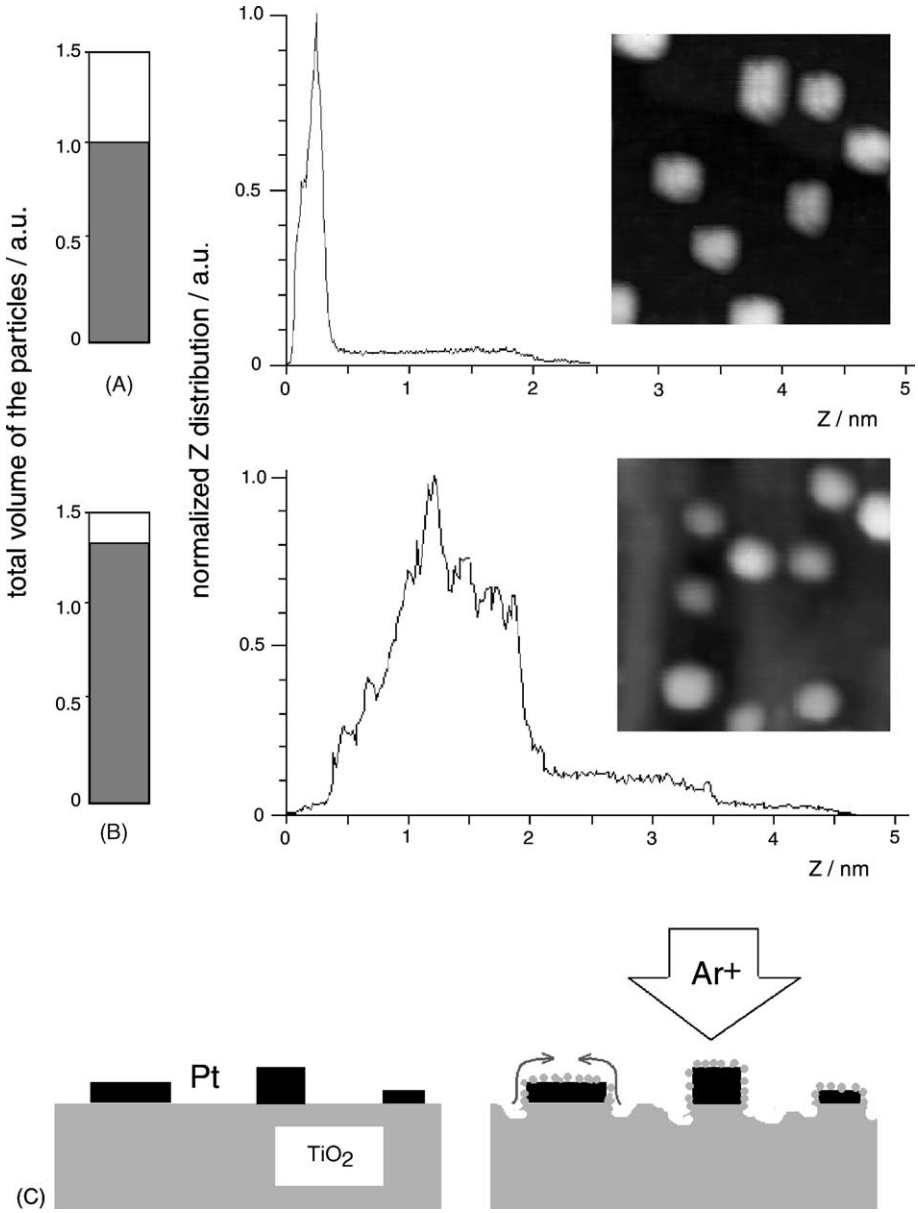

Fig. 3. The change of the z-distribution of the points on the STM images (50 nm × 50 nm) recorded (A) before and (B) after 1 min Ar^+ bombardment. The total volume of the particles is shown by bar diagrams (left). (C) The scheme suggested for the surface restructuring process.

corrugation of 1.2 nm only slightly changes (maximum up to 1.7 nm) on the effect of the ion treatment.

Fig. 3A shows the height distribution (histogram) for a characteristic region of 50 nm × 50 nm (inserted image) before the bombardment. The low height (z) values (below 0.5 nm) mean the terrace sites, the long tail in the region of 1.0–2.5 nm is characteristic for the crystallites. Totally different z-distribution appears after 1 min Ar^+ sputtering (1.5 keV, 3×10^{15} ion cm^{-2}) at 1100 K: the distribution is expanded up to 5 nm (more than twice of the original value) and the low level peak also became much wider (Fig. 3B). This means an enhancement of the corrugation by more than 100%. Fig. 3 also shows the increase (approximately 30%) of the total volume of the particles by bar diagrams. The STM images inserted in Fig. 3 were used as basis of these calculations.

The STM image of 50 nm × 50 nm recorded after 1 min Ar^+ bombardment was also analysed by plotting of some characteristic z-profile lines (Fig. 4). Three different lines are plotted: (A) in the direction of a ditch containing three particles; (B) across upper and lower terraces; and (C) across two nanoparticles localized in the lower and the upper terraces. The particles sitting in the ditches exhibit a height of approximately 3 nm, which is larger than that of the original particles before the treatment (approximately 1.5 nm). The depth of the ditches is approximately 1.5 nm, which means at least 5–6 atomic layers of the support oxide. The detailed analysis of the particle positions and the valley morphology has shown: (i) the valleys formed in the terraces are oriented in the [0 0 1] orientation (see also STM image in Fig. 1B); about 75% of the nanoparticles are located in the ditches appearing as dark areas in the STM images; (ii) the efficiency of the sputtering increased by a factor of 2–3 in the presence of the Pt crystallites. In Fig. 3C a scheme of the restructuring of the surface is suggested on the basis of the results presented above.

For the interpretation of the effect of the supported Pt nanoparticles on the Ar^+ treatment of the TiO_2(1 1 0) surface, the following should be taken into account. As it is well known, there is an effective chemical driving force for decorating of the supported Pt nanoparticles by some reduced phase of the support [6–10]. During the ion sputtering the decorating layer is continuously removed which accelerates the diffusion process on the top of the particles. At the same time the atomic diffusion of the TiO_2(1 1 0) surface is also activated by the continuous ion-activated reduction of the surface. One further factor is the more efficient sputtering from the top of the prominent crystallites. The different rates of these processes sensitively influence the morphology resulted. It can be assumed that the formation of the anisotropic ditches on the effect of the ion treatments may be explained by the anisotropic atomic diffusion rates on the TiO_2(1 1 0) surface. According to our calculations, the sputtering efficiency was increased by the factor of 2–3. This value can be much higher in the neighbourhood of the Pt nanoparticles. In other words, this effect makes it possible to sputter a TiO_2 sample in a laterally resolved manner. Considering that the tailored (distribution and size) fabrication of the metal nanoparticles is possible, it seems to be a real aim to work out a method for the fabrication of nanopits in tailored distribution, too.

In order to decrease the complicating effects of the neighbouring particles and to see how a single particle influences the morphology of the oxide support, it is needed to grow Pt nanoparticles in a very large separation. The method ('seeding + - growing') described above is suitable to achieve this aim. The images presented in Fig. 5A and B exhibit a TiO_2(1 1 0) surface containing approximately only a single Pt nanoparticle in each 100 nm × 100 nm area. To fabricate this particle arrangement, the clean TiO_2(1 1 0) surface was exposed to approximately 0.003 ML Pt at room temperature, followed by annealing in UHV (10 min) and a further deposition of Pt (approximately 0.10 ML) at 1100 K. Both images indicate that the particles are connected to the nearest upper terraces by a material bridge (a small terrace) which has a width of the same size as the diameter of the particle and which is oriented in the direction of [0 0 1]. This characteristic feature is obviously formed by the preferential diffusion of the TiO_x species activated by the Pt crystallites. On the basis of several (15–20) images recorded on this surface with different magnification, it can be concluded that this feature appears characteristically when the particle is located not too far from an upper terrace step perpendicular (or at least not parallel) to the orientation of [0 0 1].

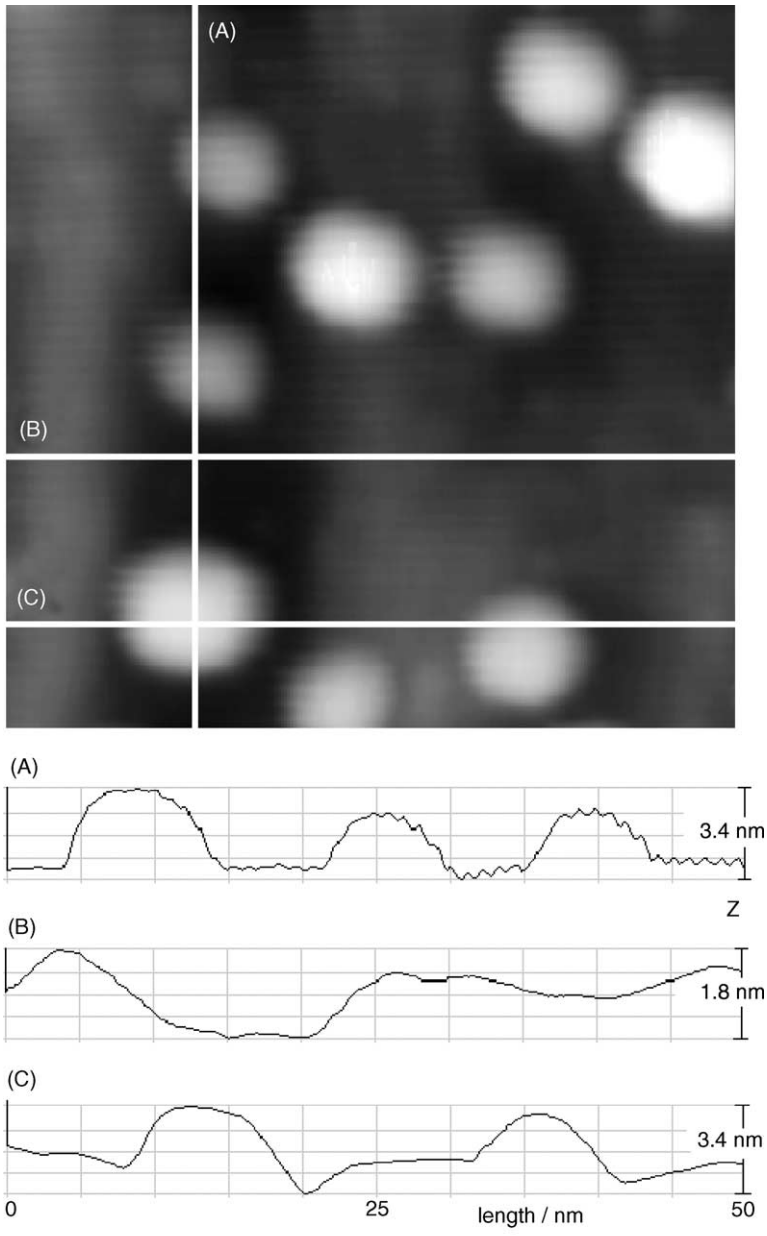

Fig. 4. Line-profile analysis of the STM image (50 nm × 50 nm) described in Fig. 3B.

The diffusion rate at 1100 K is too high, subsequently, the deficient terraces produced by the sputtering of the TiO_2(1 1 0) substrate will be filled within a few seconds. In order to detect the vacancy-islands, the temperature, at which the Ar^+ bombardment and the subsequent annealing were performed, was varied in the range of 800–1100 K. Concerning the effect of the Ar^+ bombardment, the following experiments were performed: the images in Fig. 5C and D depict the surface morphology of a clean (C) and a Pt-decorated (D) TiO_2(1 1 0) imaged after 1.5 min Ar^+ bombardment at 900 K and a subsequent

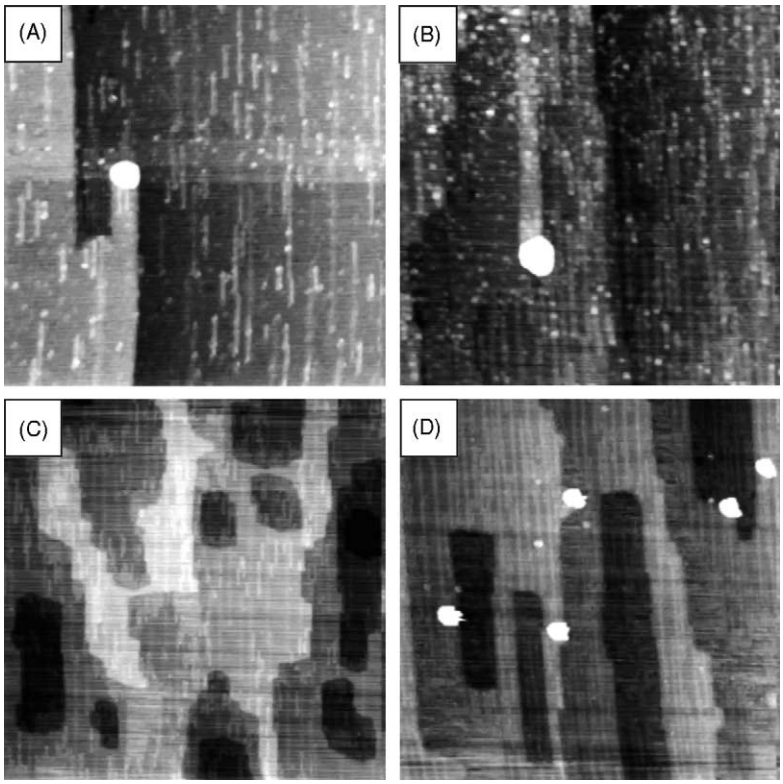

Fig. 5. (A, B) STM images of the isolated Pt crystallites of 5–6 nm grown by the 'seeding + growing' method (see text). The surface texture imaged by STM after Ar^+ treatment (1.5 min) of (C) the clean and (D) the Pt-decorated TiO_2(1 1 0)-(1 × n) surface. The size of the pictures: (A, B) 100 nm × 100 nm; (C, D) 200 nm × 200 nm.

annealing at the same temperature for 2 min. In the case of the clean surface it can be seen that the sputtering resulted in a partial removing of the outmost layer of the surface, and the size of the vacancy islands exhibit only a slight elongation in the orientation of [0 0 1] (Fig. 5C). The size of the STM image is 200 nm × 200 nm. It is worth noting that the inner ordering of the terraces needs approximately 1 min at 900 K, at the same time, these vacancy islands are very stable at this temperature (they resist even to the annealing for 10–20 min). The same treatment was also performed on a Pt-decorated surface (Fig. 5D). Before the bombardment, the surface exhibited 4–5 Pt crystallites in each 200 nm × 200 nm area and the terraces were completely ordered (Fig. 5A and B). After the bombardment, the terraces exhibited vacancy islands strongly elongated in the direction of [0 0 1] (Fig. 5D). A clear correlation between the position of the Pt nanoparticles and the nanopits was concluded on the basis of the images recorded on the different (at least 5) regions of the surface. This behaviour may be explained in the same manner as the formation of ditches in the case of higher concentration of Pt nanoparticles. The surprising feature is, however, that the particles cannot be found in the centre of the pits, in contrary, Pt particles are typically sitting in the upper terrace at the edge of the vacancy-islands. This behaviour can be explained by the activated diffusion of TiO_x species in the neighbourhood of the Pt crystallites during the post-annealing following the bombardment. It is also true that the size of the vacancy-islands can be modulated by the duration of the post-annealing.

The experiments described above were performed to prove that the supported noble metal nanoparticles can strongly influence the diffusion rate of the support surfaces (reducible oxides). In this way, the supported particles grown in a tailored distribution can be served as a template for the fabrication of nanopits in the same distribution.

4. Conclusions

The low energy (1.5 keV) Ar^+ bombardment performed at high temperatures (800–1100 K) results in a dramatic change of the corrugation of the oxide support decorated by Pt crystallites in the early stage of the treatment. This process depends largely on the surface concentration of the metal crystallites. The formation of [0 0 1] oriented ditches can be explained by taking into account the following processes: (i) an effective chemical driving force for decorating of the supported Pt nanoparticles by some reduced phase of the support; (ii) enhanced sputtering of the decorating oxide layer formed on the top of the noble metal nanoparticles; and (iii) activated surface diffusion of the TiO_2(1 1 0) due to the reduction of the support surface. It seems to be possible to work out a method for the fabrication of nanopits in tailored distribution, in which an array of supported noble metal (Pt) nanoparticles can serve as a template. The so called 'seeding + growing' method was applied in this work for growing separated Pt nanocrytallites in predetermined surface concentration and average size on the TiO_2(1 1 0)-(1 × n) substrate.

Acknowledgements

The authors gratefully acknowledge the support of the Hungarian Scientific Research Fund (OTKA) through TS40877, T046351 and T043057 projects.

References

[1] B. Navinsek, Prog. Surf. Sci. 7 (1977) 49.
[2] J.M. Fluit, S. Datz, Physica 30 (1964) 345.
[3] F.M. Lebisle, Surf. Sci. 514 (2002) 33.
[4] M.V. Ramana Murty, Surf. Sci. 500 (2002) 523.
[5] Y.-W. Chung, Practical Guide to Surface Science and Spectroscopy, Elsevier, Amsterdam, 2004.
[6] A. Berkó, I. Ulrych, K.C. Prince, J. Phys. Chem. B 102 (1998) 3379.
[7] H.P. Steinrück, F. Pesty, L. Zhang, T.E. Madey, Phys. Rev. B 51 (1995) 2427.
[8] K.D. Schierbaum, S. Fischer, M.C. Torquemada, J.L. Segovia, E. Román, J. Martin-Gago, Surf. Sci. 345 (1996) 261.
[9] O. Dulub, W. Hebenstreit, U. Diebold, Phys. Rev. Lett. 84 (16) (2000) 3646.
[10] D.R. Jennison, O. Dulub, W. Hebenstreit, U. Diebold, Surf. Sci. 492 (2001) L677.
[11] A. Berkó, G. Klivényi, F. Solymosi, J. Catal. 182 (1999) 511.
[12] A. Berkó, J. Szökő, F. Solymosi, Solid State Ionics 141–142 (2001) 197.
[13] A. Berkó, J. Szökő, F. Solymosi, Surf. Sci. 532–535 (2003) 390.
[14] S. Fischer, A.W. Munz, K.-D. Schierbaum, W. Göpel, Surf. Sci. 337 (1995) 17.
[15] I.D. Cocks, Q. Guo, E.M. Williams, Surf. Sci. 390 (1997) 119.
[16] R.E. Tanner, M.R. Castell, G.A.D. Briggs, Surf. Sci. 412–413 (1998) 672.
[17] M. Li, W. Hebenstreit, L. Gross, U. Diebold, M.A. Henderson, D.R. Jennison, P.A. Schultz, M.P. Sears, Surf. Sci. 437 (1999) 173.
[18] H. Onishi, Y. Iwasawa, Surf. Sci. 313 (1999) L783.
[19] S. Takakusagi, K.-I. Fukui, F. Nariyuki, Y. Iwasawa, Surf. Sci. 523 (2003) L41.
[20] R.A. Benett, P. Stone, N.J. Price, M. Bowker, Phys. Rev. Lett. 82 (19) (1999) 3831.